SEMARAK ILMU PUBLISHING

Journal of Advanced Research in Applied Mechanics

Journal homepage:
https://semarakilmu.com.my/journals/index.php/appl_mech/index
ISSN: 2289-7895

Triboelectric Nanogenerator Based on Tin Doped Zinc Oxide and Polyvinyl Alcohol Composite Thin Film for Energy Harvesting Applications

Dayana Kamaruzaman[1,2], Mohamad Hafiz Mamat[1,3*], Anees Abdul Aziz[1], A Shamsul Rahimi A Subki[1,4], Nurul Izzati Kamal Ariffin[1], Nurul Syafiqah Mohamed Mustakim[1], Norfarariyanti Parimon[5], N. Vasimalai[6], Mohd Hanapiah Abdullah[7], Nor Diyana Md Sin[8], Mohd Khairul Ahmad[9], Suriani Abu Bakar[10], Sandhya Pattoorpady Krishnan[11]

[1] NANO-ElecTronic Centre (NET), School of Electrical Engineering, College of Engineering, Universiti Teknologi MARA, 40450 Shah Alam, Selangor, Malaysia
[2] School of Electrical Engineering, College of Engineering, Universiti Teknologi MARA, Cawangan Terengganu, Kampus Dungun, 23000 Dungun, Terengganu, Malaysia
[3] NANO-SciTech Lab (NST), Centre for Functional Materials and Nanotechnology (FMN), Institute of Science (IOS), Universiti Teknologi MARA, 40450 Shah Alam, Selangor, Malaysia
[4] Faculty of Electrical and Electronics Engineering Technology, Universiti Teknikal Malaysia Melaka, Hang Tuah Jaya, 76100 Durian Tunggal, Melaka, Malaysia
[5] Faculty of Engineering, Universiti Malaysia Sabah, 88400 Kota Kinabalu, Sabah, Malaysia
[6] School of Physical and Chemical Sciences, B.S. Abdur Rahman Crescent Institute of Science & Technology, Vandalur, Chennai 600 048, India
[7] Center for Electrical Engineering Studies, Universiti Teknologi MARA, Cawangan Pulau Pinang, 13500 Permatang Pauh, Pulau Pinang, Malaysia
[8] School of Electrical Engineering, College of Engineering, Universiti Teknologi MARA, Cawangan Johor, Kampus Pasir Gudang, 81750 Masai, Johor, Malaysia
[9] Microelectronic and Nanotechnology Shamsuddin Research Centre, Faculty of Electrical and Electronic Engineering, Universiti Tun Hussein Onn Malaysia, 86400 Parit Raja, Johor, Malaysia
[10] Nanotechnology Research Centre, Faculty of Science and Mathematics, Universiti Pendidikan Sultan Idris, 35900 Tanjung Malim, Perak, Malaysia
[11] School of Nanoscience and Nanotechnology, Mahatma Gandhi University, Priyadarshini Hills Kottayam 686 560, Kerala, India

ARTICLE INFO

Article history:
Received 11 September 2024
Received in revised form 13 October 2024
Accepted 19 October 2024
Available online 30 October 2024

Keywords:
Triboelectric nanogenerator; Polyvinyl alcohol; Zinc oxide; Tin doping; Output voltage

ABSTRACT

The triboelectric nanogenerator (TENG) collects mechanical energy from its surroundings and converts it to electrical signals that can be used in sustainable energy harvesting technologies to help maintain the social ecosystem. However, TENG operation with pure triboelectric material may not be sufficient to power a small electronic system without modification. The optimal material capable of producing significant electrical energy with flexible structures remains a major barrier to practical application. In this study, tin-doped zinc oxide (Sn:ZnO) and polyvinyl alcohol (PVA) composite thin films were prepared using a simple solution immersion technique at various Sn atomic percentage (at.%) concentrations for use in TENG devices. The crystalline quality of a composite thin film made of Sn:ZnO and PVA was identified using x-ray diffraction. The microstructure changes of the composite thin film were found to be influenced by Sn doping, as studied using optical microscopy. The TENG with 2.5 at.% Sn:ZnO/PVA composite thin film and Kapton film achieved the highest peak voltage of 8.5 V in open circuit and 90 µW output power at 1 MΩ. The produced electrical output was then used to store energy in capacitors. According to its TENG properties, the Sn:ZnO/PVA composite thin film-based TENG has the potential to be used in low power electronic devices.

* *Corresponding author.*
E-mail address: mhmamat@uitm.edu.my

https://doi.org/10.37934/aram.126.1.165177

1. Introduction

Mechanical energy sources are ubiquitous in our daily lives, including human movement, wind, water flow, and vibration. These types of energy have the potential to be used as beneficial, environmentally friendly sources of power [1-4]. Mechanical energy to electrical energy conversion is a valuable method of harvesting energy compared to other renewable sources like solar cells, tidal, wind, and geothermal power generation [5-7]. Recent work has demonstrated the potential of harvesting mechanical energy and converting it into electricity using the triboelectric nanogenerator (TENG) [8-10]. Unlike batteries, TENG has the capability to provide a continuous supply of electricity. TENG has benefits such as low environmental impact and easy scalability in terms of size and structure. Due to its capacity to generate electrical energy from small mechanical forces like heartbeats [11], muscle movements [12], airflow [13] and raindrops [14], TENG has become a highly sought-after component of energy harvesting devices in various self-powered devices. However, most TENG encounter drawbacks like costly materials, intricate techniques, complex device architecture, and low durability. As a result, several techniques have been devised to enhance the effectiveness of TENG. These include choosing superior triboelectric materials for opposition and altering their surfaces [8, 15, 16]. Therefore, determining the optimal material that can produce significant electrical energy with flexible structures remains a major obstacle.

Zinc oxide (ZnO), a metal oxide, has been extensively utilized in nanogenerators because of its piezoelectric and triboelectric properties. It exhibits auspicious characteristics such as the ability to grow in crystalline wurtzite structures, and it can be synthesized into a wide range of morphologies, including nanobelts, nanotubes, nanowires, and nanorods [17-20]. In addition to being a semiconductor with a high exciton binding energy (60 meV) and a large direct bandgap (3.7 eV), ZnO is a biocompatible oxide because it is practically non-toxic [21, 22]. Adding certain elements to ZnO nanostructures through doping is considered an effective technique for altering their properties to meet various desired specifications [20, 23, 24]. For instance, Sn:ZnO, a doped material with improved properties over its undoped counterparts, is produced by carefully optimizing the introduction of tin (Sn) atoms to ZnO. This material maintains the desirable characteristics of ZnO, such as low toxicity, affordable production, and visible transparency for thin films [25]. Sn is considered a valuable dopant because its ionic radius closely matches that of Zn, allowing for easy replacement of Zn ions with Sn ions [26]. A variety of deposition techniques, including sol-gel [27], hydrothermal [28], spray pyrolysis [29], and solution immersion [30], were utilized to produce Sn:ZnO nanostructures. Solution immersion is one of the most preferred deposition methods due to its ability to work at a low temperature (less than 100°C), low cost, simplicity, and environmental friendliness.

Furthermore, active composite materials composed of polymers and ZnO nanostructures provide a remarkable approach to enhancing the output of nanogenerators. The utilization of ZnO nanostructures and polymer composites has been employed by scientists to boost the piezoelectric phase content within the polymer [31-33]. The use of inorganic metal oxides and polymers in composites yields superior stability and endurance. One example is the use of polydimethylsiloxane (PDMS) in ZnO composites, which are commonly used in nanogenerator applications because of their biocompatibility, flexibility, and transparency [31]. However, the manufacturing process for this composite still involves many repetitive and tedious steps. Additionally, treating the surface of PDMS requires using harmful chemicals or solvents that may damage its structural properties. Hence, polyvinyl alcohol (PVA) possesses the capacity and is well-suited for implementation in nanogenerators owing to its beneficial features. These include semi-crystalline structure, the ability to form good films, superior physical and mechanical strength, environmental friendliness,

biocompatibility, and natural breakdown [34]. PVA is frequently used in electrical devices due to its exceptional features, like its high dielectric strength and high charge storage capacity [35, 36].

In this study, a simple and cost-effective TENG constructed from Sn:ZnO and PVA (Sn:ZnO/PVA) composite thin film was prepared. The fabricated TENG consists of an aluminum electrode and Kapton film for the top triboelectric layer, and a Sn:ZnO/PVA composite film and silver electrode for the bottom triboelectric layer. The change in output voltage was investigated with the addition of Sn to the Sn:ZnO/PVA composite film. The Sn:ZnO powder was synthesized using a simple solution immersion with different at.% of Sn doping. The study aimed to explore how adding Sn to ZnO affects its ability to generate electricity and output voltage for TENG.

2. Methodology

2.1 Preparation of Sn:ZnO Powder

Zinc nitrate hexahydrate ($Zn(NO_3)_2{\cdot}6H_2O$, Friendemann Schmidt), hexamethylenetetramine (HMT, Sigma-Aldrich), and deionized (DI) water were mixed together in a beaker to prepare the ZnO powders. Different atomic percentages (at.%) of tin (II) chloride, purchased from Sigma-Aldrich, were introduced into the solution mixture, with a range of 0.5 at.% to 2.5 at.% for the Sn doping procedure. The Sn-doped ZnO solution was subjected to 30 min of sonication in an ultrasonic water bath at a temperature of 50 °C. The mixture was subjected to stirring on a hot plate at a speed of 250 rpm without the application of external heat, resulting in the formation of a white, transparent, and uniform mixture. Subsequently, the solution mixture was transferred into Schott bottles and subjected to a water bath maintained at a temperature of 95 °C for a duration of 4 h. Following the immersion process, the bottles were extracted, and the Sn:ZnO samples were meticulously transferred into a petri dish using a pipette. The samples were subsequently dehydrated in a desiccator for a few days in order to acquire the Sn:ZnO powder. Following the completion of the process, the Sn:ZnO powder was subjected to annealing for a period of 1 h in a chamber furnace at a temperature of 500 °C. Figure 1 depicts the complete procedure of the immersion method used to prepare Sn:ZnO powder.

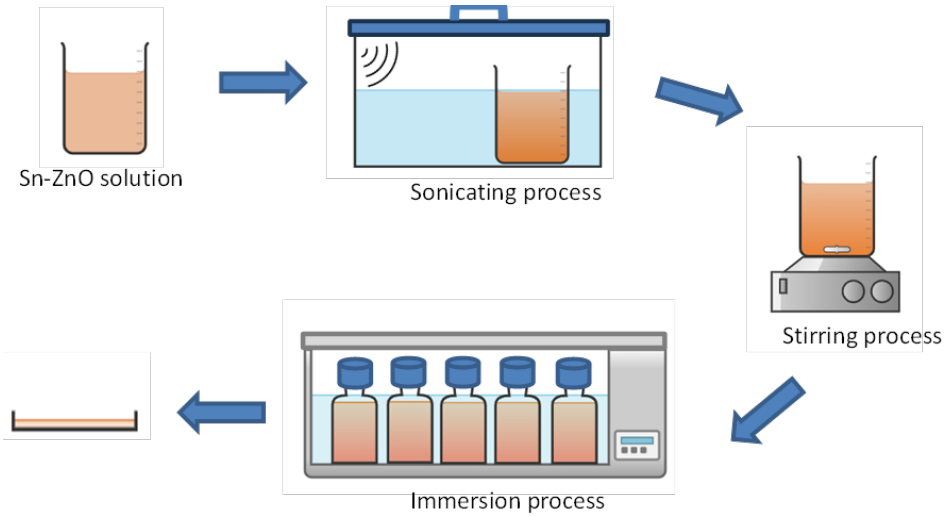

Fig. 1. The preparation process of Sn:ZnO powder using the solution immersion method

2.2 Sn:ZnO/PVA Composite Thin Film Preparation

The composite thin film was developed by mixing 1 g of Sn-doped ZnO powder with 0.5 g of PVA powder in 10 ml of DI water. The solution was then stirred at a constant speed of 300 rpm for a duration of 24 h. The composite mixture solution was subsequently transferred onto a clean glass plate using a pipette and subjected to a 24-h drying process. Once completely dried, the Sn:ZnO/PVA composite thin films were removed from the glass plate. A sample of undoped ZnO/PVA was also prepared for the purpose of comparison. Subsequently, a thermal evaporator (TE) was utilized to deposit silver (Ag) onto ZnO/PVA and Sn:ZnO/PVA composite thin films, thereby creating the Ag electrode. The resulting thin film was prepared 1×1 cm^2 in size and used as a bottom triboelectric component in constructing the TENG.

2.3 Fabrication of Sn:ZnO/PVA Composite Thin Film based TENG

To fabricate the TENG, a composite thin film of Sn:ZnO was used as an active layer. The bottom layer consisted of an Ag electrode, while the top layer was made of Kapton film with aluminum foil. These layers were adhered to a clear plastic film of the same size (1×1 cm^2) to serve as a protective cover. Then, the top and bottom layers were assembled in a vertical contact separation (VCS) configuration, in which Kapton film and Sn:ZnO/PVA composite thin film were faced opposite to one another, as illustrated in Figure 2. Kapton film and Sn:ZnO/PVA composite thin film were faced opposite to one another. Both electrodes were connected with copper wire to measure the electrical output produced by the TENG.

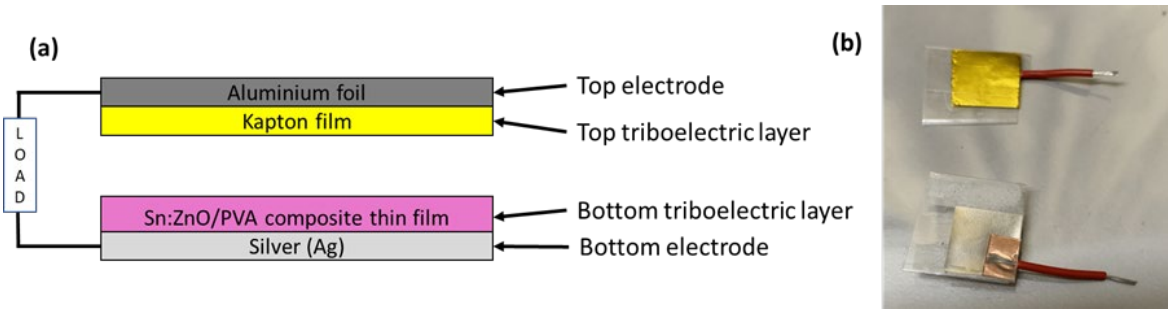

Fig. 2. Fabricated TENG device (a) the schematic diagram (b) actual images of the top and bottom triboelectric layers

2.4 Characterization

The X-ray diffraction (XRD) analysis was utilized to analyze the structural characteristics of the tin-doped zinc oxide (Sn:ZnO) composite thin film by employing Cu Kα radiation at an X-ray wavelength of 1.54 Å. The X-ray diffractograms were captured at a diffraction angle (2θ) ranging from 15° to 75°. An optical microscope (Olympus BX53M) was utilized to investigate the dispersion of Sn:ZnO powder in PVA. For the nanogenerator performance, the generation of electricity produced by the solenoid tapping system was measured using an oscilloscope (Keysight InfiniiVision DSOX2022A). Then, the fabricated TENG was linked to a rectifier to obtain the output DC voltage and was measured in a range of different connected resistors from 1 MΩ to 15 MΩ. In addition, the capacitor charging ability from the rectified output voltage was investigated by the commercially available capacitors ranging from 1 µF to 22 µF. The stored voltage in the capacitor was measured

using a digital multimeter. The dielectric measurement was performed at room temperature using the HIOKI 3552-50 LCR Hi-Tester.

3. Results

3.1 Structural Properties

Figure 3 depicts the XRD patterns of the Sn:ZnO composite thin films, where the Sn doping concentration varies in atomic percent (at.%). According to JCPDS card no. 01-075-1526, the XRD patterns indicate the existence of ZnO in the hexagonal wurtzite phase and a polycrystalline form. The patterns show nine distinct diffraction peaks at various 2θ regions, as depicted in Figure 3(a). The study revealed that the most prominent ZnO diffraction peaks were observed at 32.2° for the (100) plane, 34.8° for the (002) plane, and 36.7° for the (101) plane. The diffraction peaks observed at 47.9°, 57.0°, 63.2°, 66.9°, 68.4°, and 69.5° correspond to the planes with Miller indices (102), (110), (103), (200), (112), and (201), respectively [37]. The synthesized Sn:ZnO composite thin films have good crystallinity, which can be observed through the thin and sharp peaks. There were no discernible variations in the XRD patterns between the samples prepared with different atomic percentages of Sn doping. Furthermore, the XRD data did not show the presence of secondary phases, such as Sn clusters. This showed that Sn ions had uniformly replaced Zn ions in the ZnO matrix [38]. Based on the XRD peak, it was discovered that as the percentage of Sn doping increases, the intensity of the diffraction peaks of the (100) and (002) planes decreases slightly, indicating a gradual decrease in the crystalline quality of the thin films, proving that the ZnO lattice successfully incorporated Sn atoms [39, 40]. Figure 3(b) shows broad peaks around 20° in all composite thin films. This suggests an amorphous polymeric matrix for the PVA thin film, which is consistent with previous research [34, 41-43]. Therefore, the existence of diffraction peaks for both the ZnO and PVA peaks in the fabricated Sn:ZnO/PVA composite thin film validates the successful combination of ZnO and PVA.

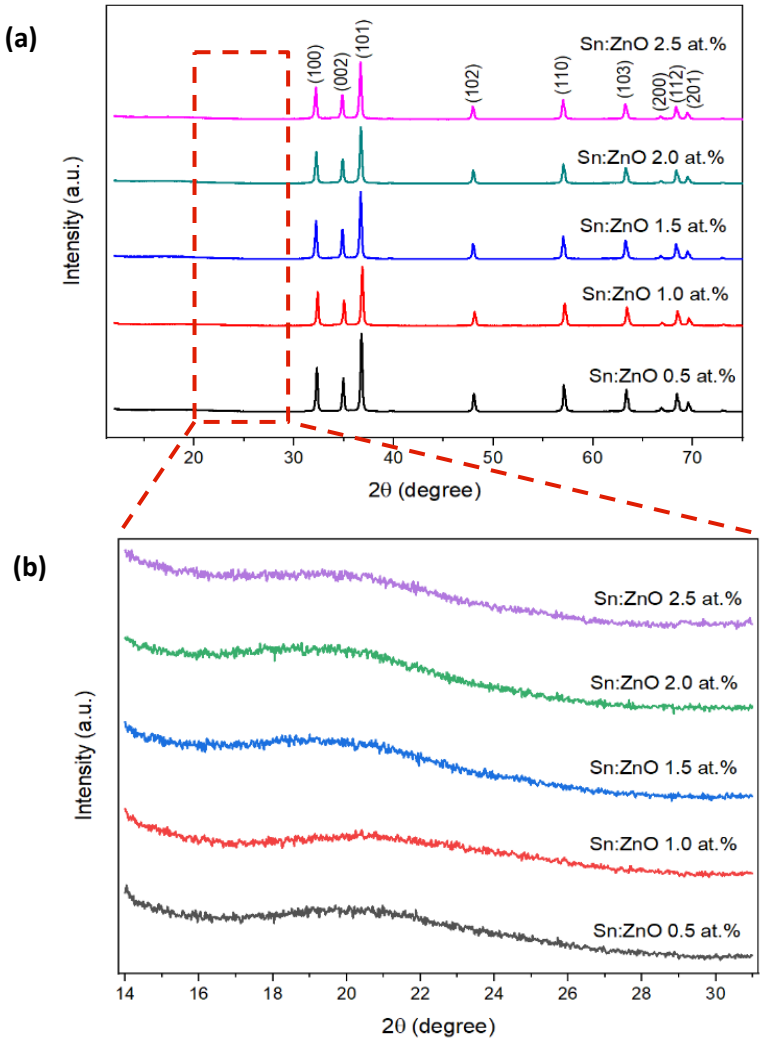

Fig. 3. XRD pattern of Sn:ZnO composite thin film (a) with different at.% of Sn doping, (b) an enlarged view of the XRD pattern for the PVA peak

3.2 Optical Microscopic Study

The morphological behavior of the synthesized composite thin films was investigated using optical microscopy. Figure 4 shows optical micrographs of ZnO/PVA and Sn:ZnO/PVA composite thin films. Figure 4(a) shows that the distribution of particles in the ZnO/PVA composite thin film was both homogeneous and agglomerative. The microstructure of the composite thin film changed significantly after the addition of Sn:ZnO to PVA. Figure 4(b)-(f) shows that the particle distribution in all Sn:ZnO/PVA composite thin films is uniform, with small and irregular shapes (in white). As the percentage of Sn doping increases, the small irregular particles become more noticeable.

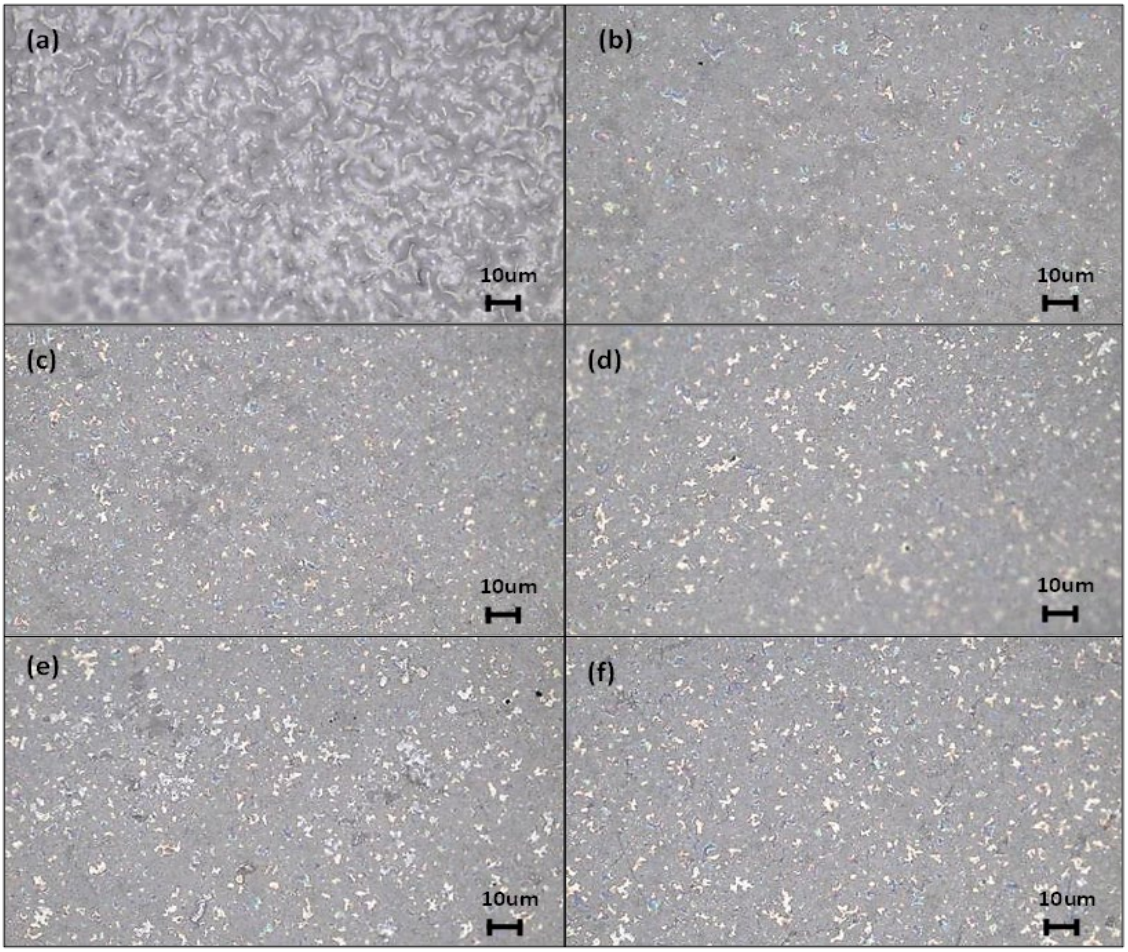

Fig. 4. Optical microscopic images of (a) ZnO/PVA thin film, (b) Sn:ZnO/PVA composite film at 0.5 at.%, (c) 1.0 at.%, (d) 1.5 at.%, (e) 2.0 at.% and (f) 2.5 at.%

3.3 Sn:ZnO Composite Thin Film based TENG Performance

The ZnO/PVA composite thin films and Sn:PVA composite thin films were used as bottom triboelectric layers in the development of the TENG device. Their capacity to generate electricity was assessed by applying an external pushing force. Here is an elucidation of the generation of the output voltage, accompanied by the schematic diagram depicted in Figure 5. Upon the application of an external force (tapping force), the Sn:ZnO/PVA composite thin film and the kapton film generated triboelectric charges as a result of the friction between the two layers. After the force had been released, the two layers were in a state of separation, resulting in the creation of a potential difference. Hence, the occurrence of a positive electric signal was observed. Once the two layers have completely divided, there is no electrical current that can pass between them, resulting in a potential difference of zero, indicating an equilibrium state. Upon exerting force to bring the layers into closer proximity once more, a detrimental electric signal was generated. The AC output signal was generated by continuously applying and releasing an external force in the contact-and-separation condition mode. Figure 6(a) illustrates the triboelectric reactions of Sn:ZnO/PVA-based TENG with varying levels of Sn doping, as well as ZnO/PVA-based TENG for comparison, using a tapping force. The ZnO/PVA TENG device attained a value of 1.5 V for the open circuit voltage (V_{oc}). The introduction of Sn doping in the 0.5 at.% Sn:ZnO/PVA TENG device led to a slight improvement in its electrical output performance, resulting in a V_{oc} value of 2.0 V. Furthermore, it was noted that as the atomic percentage of Sn doping rose, there was a substantial rise in the Voc values. The highest V_{oc} value of

8.5 V was achieved by utilizing a 2.5 at.% Sn:ZnO composite thin film in the TENG. The enhanced performance of the TENG can be attributed to an increased concentration of carriers as a consequence of Sn doping.

Prior to the utilization of the TENG device in portable electronics, it is necessary to convert the AC output signal generated by the TENG into a DC output signal. The DC output voltage is generated using a DB 107 integrated circuit (IC) rectifier, as illustrated in Figure 6(b). The full-wave rectifier converted the negative signal into a positive signal, resulting in the generation of a DC output voltage. The output power of TENG is contingent upon the external load. The electrical output of the constructed TENG was measured at various load resistances, ranging from 1 MΩ to 15 MΩ, in order to investigate the influence of external load resistance on its performance. The voltage generated by the Sn:ZnO/PVA-based TENG increased with higher load resistance, as shown in Figure 6(c). Figure 6(d) demonstrated a reverse correlation between the output current of these TENGs and the load resistance, thus confirming the principles of Ohm's law. Subsequently, the output power values of these TENGs were calculated and plotted in Figure 6(e) by utilizing the formula $P = V^2/R$, where P represents power, V represents voltage, and R represents load resistance. The TENG, fabricated using 2.5 at.% Sn:ZnO and PVA, demonstrated a maximum output power of 90 µW when connected to a 1 MΩ load. The output power diminishes as the load resistance values increase. Figure 6(f) illustrates the charging behaviour of a capacitor in a TENG, where the capacitor values are varied. This TENG utilizes a 2.5 at.% Sn:ZnO/PVA composite thin film. The capacitors were charged utilizing the DC voltage produced by the TENG when linked to a rectifier. The charging process lasted for a total of 2 min, with intervals of 25-s between each charge. Smaller capacitor values exhibited a significantly higher rate of change. After a charging period of only 2 min, a 1 µF capacitor reached its peak voltage of 2.8 V. The behavior of the TENG with different capacitance values aligns with results reported in the literature [44, 45].

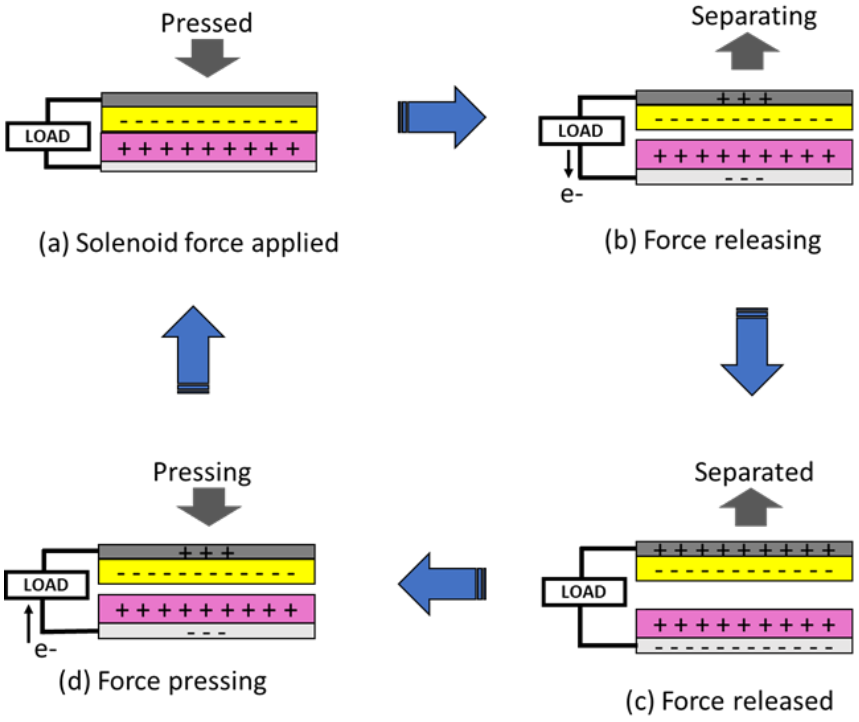

Fig. 5. Schematic diagram of the working principle of Sn:ZnO/PVA TENG

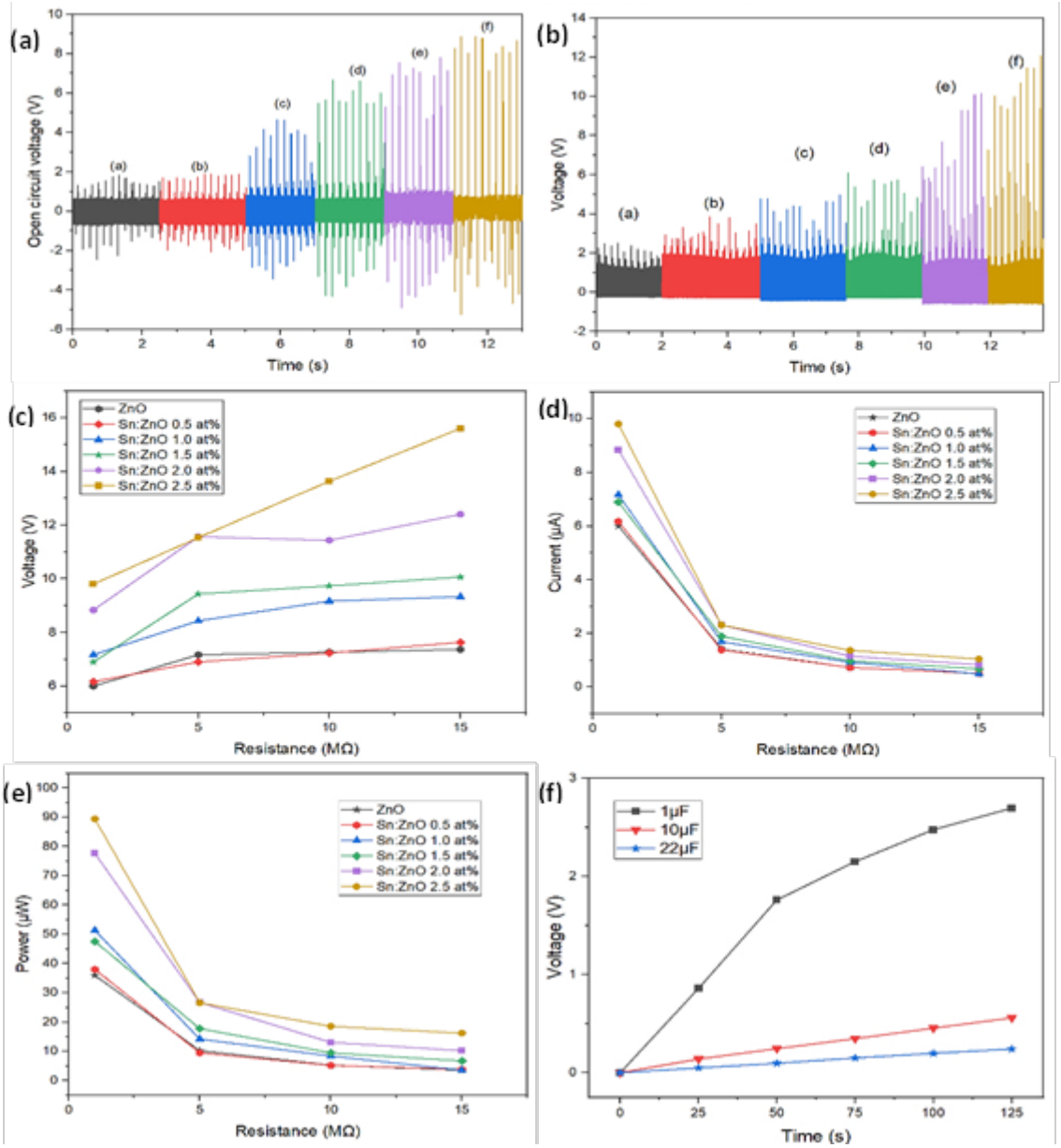

Fig. 6. Sn:ZnO/PVA TENG performance of (a) Open circuit voltage vs time (b) rectifying graph (c) voltage vs load resistance (d) current vs load resistance (e) produced power vs load resistance and (f) capacitor charging characteristic

Furthermore, the efficiency of TENG output relies on the relative permittivity of the triboelectric layers. The dielectric properties of ZnO/PVA composite films were assessed at different at.% concentrations of Sn doping. The capacitance of Sn:ZnO/PVA composite films was measured using an LCR meter across a range of frequencies (500 Hz to 100 kHz). The samples were confined within a parallel plate capacitor during the measurements. The relative permittivity was determined by applying Eq. (1) [34].

$$\varepsilon = \frac{Cd}{A\varepsilon_0} \quad (1)$$

Here, ε represents the calculated relative permittivity, C denotes the capacitance value, and d represents the distance between the two parallel plates. Meanwhile, ε_0 denotes the permittivity of the free space, while A represents the cross-sectional area of the plates. Figure 7 illustrates the

correlation between the frequency and the relative permittivity of the Sn:ZnO/PVA composite thin films. The composite films exhibited an increase in relative permittivity with an increase in the at.% concentrations of Sn doping. Incorporating Sn doping into the Sn:ZnO/PVA composite improves the relative permittivity of the material, resulting in an augmentation of the surface charge density in the composite films. This leads to a substantial augmentation in triboelectric charges throughout the process of contact and separation [46].

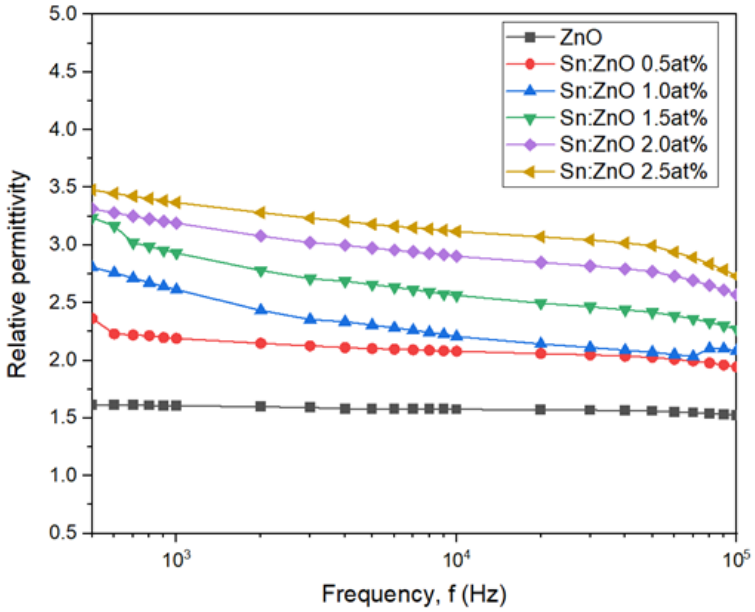

Fig. 7. Dielectric constants of the Sn:ZnO/PVA composite films at various at% Sn doping with frequency.

4. Conclusions

The Sn:ZnO powder was successfully synthesized using a simple solution immersion method with various at.% amounts of Sn doping and used as a triboelectric layer in TENG device fabrication. The XRD results showed the presence of ZnO and PVA peaks, confirming the successful composite thin film. Furthermore, the crystallinity of the Sn:ZnO/PVA composite thin film decreased as the at.% concentration of Sn doping into ZnO increased, indicating that the ZnO lattice was successfully incorporated with Sn ions. The optical micrograph depicts the alterations in the microstructure upon the introduction of Sn:ZnO into PVA. An increase in the at.% concentration of Sn doping led to the formation of a greater number of small, irregular particles in the film. Furthermore, the Sn:ZnO/PVA-based TENG produced more electricity than the ZnO/PVA-based TENG due to the higher carrier concentration triggered by Sn doping. The V_{oc} value was increased by increasing the percentage of Sn doping. The 2.5 at.% Sn:ZnO composite thin film-based TENG achieved the highest V_{oc} value of 8.5 V, with an output power of 90 µW at 1 MΩ. Furthermore, as the amount of Sn doping in ZnO/PVA composites increased, the relative permittivity of the Sn:ZnO/PVA composite film improved. The addition of Sn doping in the ZnO/PVA composite thin film had a substantial impact on the structural, morphological, and output performance of the TENG device.

Acknowledgement
This research was funded by Strategic Research Partnership (SRP) grant (100-RMC 5/3/SRP INT (020/2022)) of UiTM Shah Alam. The authors acknowledged the Pejabat TNCPI UiTM for the funding.

References

[1] Yinghong Wu, Yang Luo, Jingkui Qu, Walid A. Daoud, and Tao Qi. "Liquid single-electrode triboelectric nanogenerator based on graphene oxide dispersion for wearable electronics." *Nano Energy* 64 (2019): 103948. https://doi.org/10.1016/j.nanoen.2019.103948.

[2] Dong Liu, Jinmei Liu, Maosen Yang, Nuanyang Cui, Haoyu Wang, Long Gu, Longfei Wang, and Yong Qin. "Performance enhanced triboelectric nanogenerator by taking advantage of water in humid environments." *Nano Energy* 88 (2021): 106303. https://doi.org/10.1016/j.nanoen.2021.106303.

[3] Xinyue Wu, Xunjia Li, Jianfeng Ping, and Yibin Ying. "Recent advances in water-driven triboelectric nanogenerators based on hydrophobic interfaces." *Nano Energy* 90 (2021): 106592. https://doi.org/10.1016/j.nanoen.2021.106592.

[4] Lokesh Dhakar, Prakash Pitchappa, Francis Eng Hock Tay, and Chengkuo Lee. "An intelligent skin based self-powered finger motion sensor integrated with triboelectric nanogenerator." *Nano Energy* 19 (2016): 532-540. https://doi.org/10.1016/j.nanoen.2015.04.020.

[5] Young Pyo Jeon, Chaoxing Wu, Keon-Ho Yoo, and Tae Whan Kim. "Enhancement of the output voltage for triboelectric nanogenerators due to Al doping in the zinc oxide layer." *Journal of Alloys and Compounds* 831 (2020): 154913. https://doi.org/10.1016/j.jallcom.2020.154913.

[6] Yaakob Yusli, Basri Mahamad Hisyam Mahamad, Bardzan Muhammad Farhan, Ismail Noor Iswadi, Razak Azli Abd, and Pahmi Muhammad Arif Ab Hamid. "The Stability Analysis Of Floating Buoy As A Wave Energy Harvester For Malaysian Coastal Area." *Journal of Advanced Research in Applied Mechanics* 96, no. 1 (2022): 1-6. https://doi.org/10.37934/aram.96.1.16.

[7] Alotaibi Alowaid, Muda Mohd Khairul Hafiz, Mustapha Faizal, Halin Izhal Abdul, and Yidris Noorfaizal. "Perpetual Motion Wind Turbine Generator for Novelty Energy Harvesting System; Conceptual Design Approach." *Journal of Advanced Research in Fluid Mechanics and Thermal Sciences* 94, no. 2 (2022): 166-173. https://doi.org/10.37934/arfmts.94.2.166173.

[8] Aihua Chen, Chen Zhang, Guang Zhu, and Zhong Lin Wang. "Polymer Materials for High-Performance Triboelectric Nanogenerators." *Advanced Science* 7, no. 14 (2020): 2000186. https://doi.org/10.1002/advs.202000186.

[9] Changsheng Wu, Aurelia C. Wang, Wenbo Ding, Hengyu Guo, and Zhong Lin Wang. "Triboelectric Nanogenerator: A Foundation of the Energy for the New Era." *Advanced Energy Materials* 9, no. 1 (2019): 1802906. https://doi.org/10.1002/aenm.201802906.

[10] Aifang Yu, Yaxing Zhu, Wei Wang, and Junyi Zhai. "Progress in Triboelectric Materials: Toward High Performance and Widespread Applications." *Advanced Functional Materials* 29, no. 41 (2019): 1900098. https://doi.org/10.1002/adfm.201900098.

[11] Gunasekhar, R., and A. Anand Prabu. "Polyvinylidene fluoride/aromatic hyperbranched polyester 2nd generation based triboelectric sensor for polysomnographic and health monitoring applications." *Sensors and Actuators A: Physical* 355 (2023): 114311. https://doi.org/10.1016/j.sna.2023.114311.

[12] Minseok Kang, Heejae Shin, Youngjun Cho, Jaewoo Park, Pritish Nagwade, and Sanghoon Lee. "Triboelectric neurostimulator for physiological modulation of leg muscle." *Nano Energy* 103 (2022): 107861. https://doi.org/10.1016/j.nanoen.2022.107861.

[13] Yingchun Wu, Yushen Hu, Ziyu Huang, Chengkuo Lee, and Fei Wang. "Electret-material enhanced triboelectric energy harvesting from air flow for self-powered wireless temperature sensor network." *Sensors and Actuators A: Physical* 271 (2018): 364-372. https://doi.org/10.1016/j.sna.2017.12.067.

[14] Jingbo Yuan, Xiya Yang, Duo Zheng, Jiangtao Guo, Weize Lin, Jiawei Liao, Yudi Wang, L. Vaillant-Roca, Jialong Duan, and Qunwei Tang. "Perovskite quantum dot-based tandem triboelectric-solar cell for boosting the efficiency and rain energy harvesting." *Nano Energy* 110 (2023): 108341. https://doi.org/10.1016/j.nanoen.2023.108341.

[15] Chakradhar, R. P. S., V. Dinesh Kumar, J. L. Rao, and Bharathibai J. Basu. "Fabrication of superhydrophobic surfaces based on ZnO–PDMS nanocomposite coatings and study of its wetting behaviour." *Applied Surface Science* 257, no. 20 (2011): 8569-8575. https://doi.org/10.1016/j.apsusc.2011.05.016.

[16] Kumarjyoti Roy, Md Alam, Swapan Mandal, and Subhas Debnath. "Surface modification of sol–gel derived nano zinc oxide (ZnO) and the study of its effect on the properties of styrene–butadiene rubber (SBR) nanocomposites." *Journal of nanostructure in chemistry* 4 (2014): 133-142. https://doi.org/10.1007/s40097-014-0127-9.

[17] Ali Dad Chandio, Muhammad Saleem, Hasan Raza Khan, Iqra Naeem Hyder, and Maryam Ali. "Modified Zinc Oxide Nanoparticles for Corrosion Resistance Applications." *Journal of the Chemical Society of Pakistan* 42 (2020): 705. https://doi.org/10.52568/000686/JCSP/42.05.2020.

[18] Zaidatul Hanis Azmi, Siti Nurnadiah Mohd Aris, Shamsu Abubakar, Suresh Sagadevan, Rikson Siburian, and Suriati Paiman. "Effect of Seed Layer on the Growth of Zinc Oxide Nanowires by Chemical Bath Deposition Method." *Coatings* 12, no. 4 (2022): 474. https://doi.org/10.3390/coatings12040474.

[19] Mamat, Mohamad Hafiz, Mohd Izzudin Che Khalin, Nik Noor Hafizah Nik Mohammad, Zuraida Khusaimi, Nor Diyana Md Sin, Shafinaz Sobihana Shariffudin, Musa Mohamed Zahidi, and Mohamad Rusop Mahmood. "Effects of Annealing Environments on the Solution-Grown, Aligned Aluminium-Doped Zinc Oxide Nanorod-Array-Based Ultraviolet Photoconductive Sensor." *Journal of Nanomaterials* 2012, no. 1 (2012): 189279. https://doi.org/10.1155/2012/189279

[20] Abdullah, M. A. R., M. H. Mamat, A. S. Ismail, M. F. Malek, A. B. Suriani, M. K. Ahmad, IB Shameem Banu, R. Amiruddin, and M. Rusop. "Direct and seedless growth of Nickel Oxide nanosheet architectures on ITO using a novel solution immersion method." *Materials Letters* 236 (2019): 460-464. https://doi.org/10.1016/j.matlet.2018.10.163.

[21] Sanusi Saedah Munirah, Ruziana Mohamed, Malek Mohd Firdaus, Ahmad Nurin Jazlina, and Mahmood Mohamad Rusop. "Enhanced The Properties of ZnO Thin Film by Graphene Oxide for Dye Sensitized Solar Cell Applications." *Journal of Advanced Research in Fluid Mechanics and Thermal Sciences* 100, no. 3 (2022): 171-181. https://doi.org/10.37934/arfmts.100.3.171181.

[22] Akhilesh Kumar Gupta, Chih-Hsien Hsu, Sz-Nian Lai, and Chao-Sung Lai. "ZnO-Polystyrene Composite as Efficient Energy Harvest for Self-Powered Triboelectric Nanogenerator." *ECS Journal of Solid State Science and Technology* 9, no. 11 (2020): 115019. https://doi.org/10.1149/2162-8777/aba7fa.

[23] Malek, M. F., M. Z. Sahdan, M. H. Mamat, M. Z. Musa, Z. Khusaimi, S. S. Husairi, ND Md Sin, and M. Rusop. "A novel fabrication of MEH-PPV/Al: ZnO nanorod arrays based ordered bulk heterojunction hybrid solar cells." *Applied Surface Science* 275 (2013): 75-83. https://doi.org/10.1016/j.apsusc.2013.01.119.

[24] Subki, A. Shamsul Rahimi A., Mohamad Hafiz Mamat, Musa Mohamed Zahidi, Mohd Hanapiah Abdullah, I. B. Shameem Banu, Nagamalai Vasimalai, Mohd Khairul Ahmad et al. "Optimization of aluminum dopant amalgamation immersion time on structural, electrical, and humidity-sensing attributes of pristine ZnO for flexible humidity sensor application." *Chemosensors* 10, no. 11 (2022): 489. https://doi.org/10.3390/chemosensors10110489.

[25] Al-Khalli, N., M. Hezam, M. Alduraibi, and M. Abdel-Rahman. "Tuning of zinc oxide temperature sensing and optical absorption properties by tin heavy-doping." *Materials Science in Semiconductor Processing* 133 (2021): 105988. https://doi.org/10.1016/j.mssp.2021.105988.

[26] Ismail, A. S., M. H. Mamat, I. B. Shameem Banu, M. F. Malek, M. M. Yusoff, R. Mohamed, W. R. W. Ahmad et al. "Modulation of Sn concentration in ZnO nanorod array: intensification on the conductivity and humidity sensing properties." *Journal of Materials Science: Materials in Electronics* 29 (2018): 12076-12088. https://doi.org/10.1007/s10854-018-9314-7.

[27] Berumen-Torres, J. A., J. G. Quiñones-Galvan, H. Durán-Muñoz, C. H. Guzmán, G. Torres-Delgado, J. J. Ortega-Sigala, J. J. Araiza-Ibarra, and R. Castanedo-Pérez. "Low resistivity annealed tin-doped zinc oxide thin films prepared by the sol gel technique." *Materials Science and Engineering: B* 268 (2021): 115134. https://doi.org/10.1016/j.mseb.2021.115134.

[28] Priyadharsan, A., S. Shanavas, C. Vidya, J. Kalyana Sundar, R. Acevedo, and P. M. Anbarasan. "Structural and optical properties of Sn doped ZnO-rGO nanostructures using hydrothermal technique." *Materials Today: Proceedings* 26 (2020): 3522-3525. https://doi.org/10.1016/j.matpr.2019.05.440.

[29] Vasanthi, M., K. Ravichandran, N. Jabena Begum, G. Muruganantham, S. Snega, A. Panneerselvam, and P. Kavitha. "Influence of Sn doping level on antibacterial activity and certain physical properties of ZnO films deposited using a simplified spray pyrolysis technique." *Superlattices and Microstructures* 55 (2013): 180-190. https://doi.org/10.1016/j.spmi.2012.12.011.

[30] Mamat, M. H., A. S. Ismail, N. Parimon, N. Vasimalai, M. H. Abdullah, M. F. Malek, M. K. Yaakob et al. "Heterojunction of SnO2 nanosheet/arrayed ZnO nanorods for humidity sensing." *Materials Chemistry and Physics* 288 (2022): 126436. https://doi.org/10.1016/j.matchemphys.2022.126436.

[31] Kriti Batra, Nidhi Sinha, and Binay Kumar. "Ba-doped ZnO nanorods: Efficient piezoelectric filler material for PDMS based flexible nanogenerator." *Vacuum* 191 (2021): 110385. https://doi.org/10.1016/j.vacuum.2021.110385.

[32] Jeeju, P. P., and S. Jayalekshmi. "On the interesting optical properties of highly transparent, thermally stable, spin-coated polystyrene/zinc oxide nanocomposite films." *Journal of applied polymer science* 120, no. 3 (2011): 1361-1366. https://doi.org/10.1002/app.33188.

[33] Andreia dos Santos, Filipe Sabino, Ana Rovisco, Pedro Barquinha, Hugo Águas, Elvira Fortunato, Rodrigo Martins, and Rui Igreja. "Optimization of ZnO Nanorods Concentration in a Micro-Structured Polymeric Composite for Nanogenerators." *Chemosensors* 9, no. 2 (2021): 27. https://doi.org/10.3390/chemosensors9020027.

[34] Althubiti, N. A., A. Atta, E. Abdeltwab, Nuha Al-Harbi, and M. M. Abdel-Hamid. "Structural characterization and dielectric properties of low energy hydrogen beam irradiated PVA/ZnO nanocomposite materials." *Inorganic Chemistry Communications* 153 (2023): 110779. https://doi.org/10.1016/j.inoche.2023.110779.

[35] Mymona Mohsen AbutalibAbdulwahab Rajeh. "Boosting optical and electrical characteristics of polyvinyl alcohol/carboxymethyl cellulose nanocomposites by GNPs/MWCNTs fillers as an application in energy storage devices." *International Journal of Energy Research* 46, no. 5 (2022): 6216-6224. https://doi.org/10.1002/er.7559.

[36] Haifa Mohammed AlghamdiAbdulwahab Rajeh. "Synthesis of carbon nanotubes/titanium dioxide and study of its effect on the optical, dielectric, and mechanical properties of polyvinyl alcohol/sodium alginate for energy storage devices." *International Journal of Energy Research* 46, no. 14 (2022): 20050-20066. https://doi.org/10.1002/er.7578.

[37] Subki, A. S. R. A., Mohamad Hafiz bin Mamat, M. Z. Musa, M. H. Abdullah, IB Shameem Banu, N. Vasimalai, M. K. Ahmad et al. "Effects of varying the amount of reduced graphene oxide loading on the humidity sensing performance of zinc oxide/reduced graphene oxide nanocomposites on cellulose filter paper." *Journal of Alloys and Compounds* 926 (2022): 166728. https://doi.org/10.1016/j.jallcom.2022.166728.

[38] Yildiz, A. B. D. U. L. L. A. H., T. Serin, E. L. İ. F. Öztürk, and N. Serin. "Barrier-controlled electron transport in Sn-doped ZnO polycrystalline thin films." *Thin solid films* 522 (2012): 90-94. https://doi.org/10.1016/j.tsf.2012.09.006.

[39] Ismail, A. S., M. H. Mamat, ND Md Sin, M. F. Malek, A. S. Zoolfakar, A. B. Suriani, A. Mohamed, M. K. Ahmad, and M. Rusop. "Fabrication of hierarchical Sn-doped ZnO nanorod arrays through sonicated sol− gel immersion for room temperature, resistive-type humidity sensor applications." *Ceramics International* 42, no. 8 (2016): 9785-9795. https://doi.org/10.1016/j.ceramint.2016.03.071.

[40] Thirumoorthi, M., and J. Thomas Joseph Prakash. "Doping effects on physical properties of (1 0 1) oriented tin zinc oxide thin films prepared by nebulizer spray pyrolysis method." *Materials Science and Engineering: B* 248 (2019): 114402. https://doi.org/10.1016/j.mseb.2019.114402.

[41] Ghadeer Abdul Hadi Abdul Jabbar, Asrar Abdulmunem Saeed, and Mahasin F. Hadi Al-Kadhemy. "Optical characteristics and bacterial-resistance ability of PVA/ZnO nanocomposites." *Kuwait Journal of Science* (2023): https://doi.org/10.1016/j.kjs.2023.03.004.

[42] Mohammad Ali Norouzi, Majid Montazer, Tina Harifi, and Pegah Karimi. "Flower buds like PVA/ZnO composite nanofibers assembly: Antibacterial, in vivo wound healing, cytotoxicity and histological studies." *Polymer Testing* 93 (2021): 106914. https://doi.org/10.1016/j.polymertesting.2020.106914.

[43] Varsha Viswanath, Sreeja Sreedharan Nair, Subodh G, and C. I. Muneera. "Zinc oxide encapsulated poly (vinyl alcohol) nanocomposite films as an efficient third-order nonlinear optical material: Structure, microstructure, emission and intense low threshold optical limiting properties." *Materials Research Bulletin* 112 (2019): 281-291. https://doi.org/10.1016/j.materresbull.2018.12.022.

[44] Harishkumarreddy Patnam, Bhaskar Dudem, Sontyana Adonijah Graham, and Jae Su Yu. "High-performance and robust triboelectric nanogenerators based on optimal microstructured poly(vinyl alcohol) and poly(vinylidene fluoride) polymers for self-powered electronic applications." *Energy* 223 (2021): 120031. https://doi.org/10.1016/j.energy.2021.120031.

[45] Muhammad Umaid Bukhari, Memoon Sajid, Muhammad Qasim Mehmood, Muhammad Zubair, and Kashif Riaz. *Facile and Cost Effective Paper Based Triboelectric Nanogenerators for Self Powered Environmental Sensing System*. 2020 International Conference on UK-China Emerging Technologies (UCET), Glasgow, UK, pp. 1-4, 2020. https://doi.org/10.1109/UCET51115.2020.9205356.

[46] Sarbaranjan Paria, Suman Kumar Si, Sumanta Kumar Karan, Amit Kumar Das, Anirban Maitra, Ranadip Bera, Lopamudra Halder, Aswini Bera, Anurima De, and Bhanu Bhusan Khatua. "A strategy to develop highly efficient TENGs through the dielectric constant, internal resistance optimization, and surface modification." *Journal of Materials Chemistry A* 7, no. 8 (2019): 3979-3991. https://doi.org/10.1039/C8TA11229K.